Wormlike Micelles of Block Copolymers: Measuring the Linear Density by AFM and Light Scattering

Isaac LaRue, Mireille Adam,* Marcelo da Silva, Sergei S. Sheiko,* and Michael Rubinstein

Department of Chemistry, University of North Carolina at Chapel Hill, Chapel Hill, North Carolina 27599-3290

Received January 22, 2004; Revised Manuscript Received April 22, 2004

ABSTRACT: Wormlike micelles can form from polystyrene-*b*-polyisoprene copolymers in heptane—a selective solvent for polyisoprene. We have measured the aggregation number per unit length of polystyrene-*b*-polyisoprene wormlike micelles by light scattering and AFM. The values obtained from both techniques are in good agreement. The aggregation number per unit length decreases as the temperature increases due to the improvement of the solvent quality.

Introduction

When diblock polymers are placed in a selective solvent (good/Θ solvent for one block and poor/nonsolvent for the other), the diblocks will aggregate and form micelles above a certain concentration, called the critical micelle concentration.[1−5] By forming micelles, the diblocks lower their free energy. The insoluble blocks will form the core of the micelle, and the soluble blocks form the corona to keep the micelles in solution. To determine the size and shape of the micelles, one must balance the free energy of the core−solvent interface with the free energies of the corona and the core.[6] If the soluble block is longer than the insoluble block, spherical micelles will form.[7,8] Under these conditions, the size and aggregation number of the micelle are determined by balancing the free energy of the interface with the free energy of the corona. Changes in the free energy of the core (due to changes in the size or aggregation number of the micelle) are relatively small and do not have to be included when calculating the size or aggregation number of spherical micelles. As the length of the soluble block is reduced, while keeping the insoluble block constant, the aggregation number of the micelles will increase, and the thickness of the corona decreases, eventually becoming less than the radius of the core. When this is the case, the corona can be viewed as a planar brush, and the micelles have been called "crew-cut".[9] Throughout the "crew-cut" region, the free energy of the interface is still balanced almost exclusively by the free energy of the corona; however, in part of this region, the micelles can further lower their free energies by changing their shape from spherical to cylindrical.

To understand the shape change, one should consider a small correction to the overall free energy due to the curvature of the corona and compare them with the elastic energy of the core blocks.[10] Although the corona of the micelle is viewed as a planar brush, the brush actually is slightly curved. The higher the curvature, the more space there is for the corona blocks and the more stretched the core blocks become. At a constant surface area per diblock, the corona blocks prefer smaller micelles with a high curvature, while the core blocks prefer large micelles with a low curvature. When decreasing the length of the corona block, the negative corrections (due to curvature) to the free energy of the corona eventually become comparable to the increase in the free energy of the core. At this point, the spherical micelles can reduce the stretching on the core blocks by changing their shape from spheres to cylinders.[11] For a cylinder, the gain in the corona free energy due to curvature becomes less than for a sphere. However, the cylinder gains energy due to a decrease in the stretching of the core blocks. We have shown previously that by reducing the length of the corona block, while keeping the core block constant, a change from stable spherical micelles to stable cylindrical, wormlike micelles is observed.[12] While wormlike micelles have been observed previously, most observations have been for systems that have additional stabilizing forces, including blocks that are charged,[13,14] crystallizable,[15] that can form hydrogen bonds with the solvent,[16] or in cross-linked systems.[17−19] By using polystyrene-*b*-polyisoprene in dilute heptane solutions, we are looking at a noncharged, amorphous system that does not exhibit specific interactions with the solvent.

To properly study this problem, one must take into account the large variation in the size of the micelles that will be studied. Spherical micelles have been found to have diameters from 20 to 150 nm depending on the size of the blocks. As such, they lend themselves nicely to be investigated by light scattering. In contrast, cylindrical, wormlike micelles have been found to have lengths on the order of several microns. Because of their large size, we are able to study aspects of the internal structure of the micelle such as the mass per unit length; however, we are unable to study the entire wormlike micelle by light scattering. While studying the internal structure can lead to some understanding of the micelles, it is necessary to use additional techniques that are able to study the entire micelle and analyze the total length (contour length) along with the persistence length. Microscopy, such as TEM, is a technique that has been used in the past to visualize entire wormlike micelles.[13,16,20] We use atomic force microscopy (AFM), which has the added benefit of being a 3-D technique. This not only allows for visualization of the entire micelle, yielding lengths and widths of the

* To whom correspondence should be addressed: e-mail: madam@email.unc.edu, sergei@email.unc.edu.

10.1021/ma049845b CCC: $27.50
Published on Web 05/27/2004

micelles, but also allows for the determination of the thickness of the micelles, enabling calculations of the volume the micelles occupy. While AFM and other high-resolution microscopic techniques allow for visualization of the entire micelle, they have the drawback that one is looking at the micelles adsorbed onto a surface rather than in solution. In this paper we will investigate the linear density of wormlike micelles and compare the results measured by light scattering in solution and by AFM in a dry state adsorbed onto a surface.

Experimental Section

Materials. Polystyrene-*b*-polyisoprene diblock copolymer with a 42K PS block and a 10K PI block, denoted as sample 40−10, was purchased from Polymer Source Inc. The diblock was characterized by a static and dynamic light scattering in cyclohexane and gel permeation chromatography in THF to verify the M_W and to ensure that there was no PS homopolymer. Since cyclohexane is a Θ solvent for PS, any residual homopolymer would aggregate at low temperatures and could be easily detected by light scattering (see Supporting Information). All solvents were purchased from Fisher Chemicals or Acros Organics and were filtered through 0.2 μm NALGENE PTFE filters, to remove any dust particles, prior to use.

Sample Preparation. Using filtered solvent, all diblock sample solutions, prepared by weighing, were placed under argon and allowed to equilibrate at 60 °C for ∼24 h and then slowly cooled to room temperature (∼5°/h). The resulting solution was then allowed to equilibrate at the temperature of interest for at least 24 h. For AFM samples, a freshly cleaved mica substrate was dipped into the diblock solution at the temperature of interest for 5 s, removed, and allowed to dry.

Method. AFM images were collected using a Nanoscope IIIa multimode atomic force microscope (Veeco Metrology Group) in tapping mode. The scan angle was adjusted so that the micelles were running vertically for images collected for aggregation number determination. This ensured the cross-sectional area determined was perpendicular to the long axis of the wormlike micelles. The randomization of the scan angle also helped to average out any distortion caused by thermal drift, scanner hysteresis, and anisotropic tip shape. After the images had been collected, they were zoomed into the area of interests and then manually plane fit in order to ensure that the substrate was even across the image. Volumes were then obtained using the "Bearing" feature of the Nanoscope software.

Light scattering was done using a Brookhaven goniometer equipped with a Coherent argon laser using the 514 nm line, an operating power of 20−100 mW, and an angle range of 15°−155°. At low angles, a counting time of 10 s repeated once was used to get rid of the dust rejection software. Otherwise, because of large fluctuations, the software would reject all but the lowest intensity, causing the wormlike micelles to appear much shorter than was observed by AFM.

Results and Discussion

Sample 40−10 was found to exist almost exclusively as wormlike micelles with only a small fraction of spherical and donutlike micelles, as seen Figure 1. The fraction of spherical micelles seems to increase at lower temperatures. This effect will be investigated at a later time. Wormlike micelles were observed to have contour lengths from 0.2 to 12 μm with a high polydispersity, as seen in Figure 2. Most wormlike micelles were also found to have an undulated structure, and as predicted by theory, the radius of the end-caps was larger than the rest of the micelle.[21] All micelle shapes were found to have diameters that ranged between 30 and 40 nm and heights from 20 to 30 nm. Average heights and diameters of wormlike micelles prepared at different temperatures are given in Table 1.

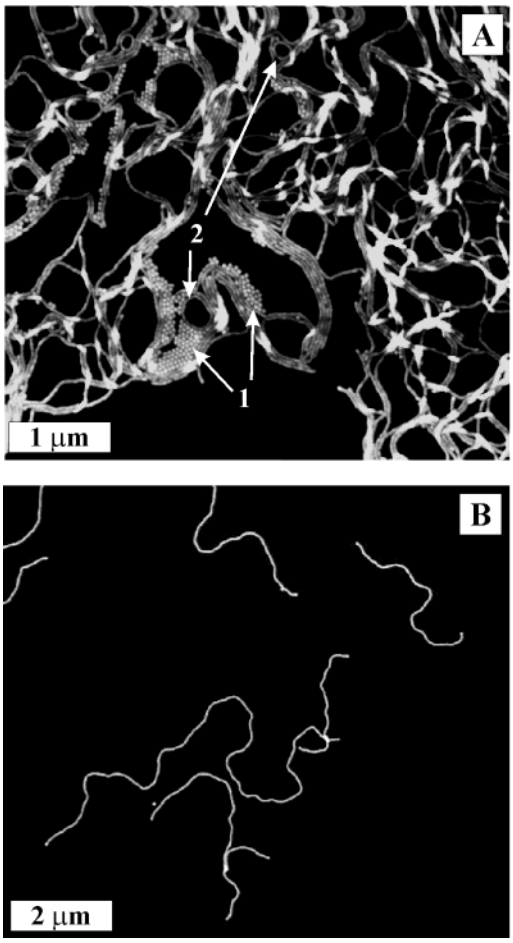

Figure 1. (A) AFM height image of 40−10 diblock adsorbed from heptane at $T = 4$ °C and a concentration of 3.4×10^{-4}g/mL shows coexistence of spherical (1), cylindrical, and donut (2) micelles, with the majority being wormlike. (B) AFM height image of 40−10 diblock adsorbed from heptane at room temperature and a concentration of 3×10^{-5}g/mL shows individual cylindrically shaped wormlike micelles.

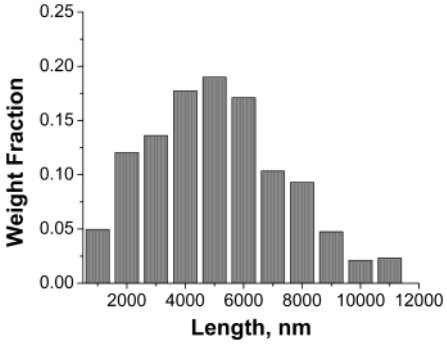

Figure 2. Length distribution of wormlike micelles at a concentration of 1.53×10^{-5}g/mL. Length average length is $L_w = 5.0$ μm with a polydispersity index of $L_w/L_n = 1.5$. The number of analyzed micelles is 332.

Aggregation Number from AFM. One known issue when using AFM is that the tips have a finite radius causing a broadening of the features.[22−25] This effect is shown in Figure 3A,B. To correctly calculate the actual cross-sectional area, the contribution from the AFM tips needs to be evaluated. This was done by taking images of multiple micelles lying side-by-side, as seen in Figure 3C. By plotting the cross-sectional area vs the number of parallel micelles, one can obtain the cross-sectional area for a single micelle from the slope and the cross-

Table 1. Average Height and Diameter of Wormlike Micelles

temperature (°C)	height (nm)	diameter (nm)[a]
23	27 ± 2	33 ± 3
40	26 ± 2	30 ± 3
60	22 ± 1	33 ± 3

[a] Diameters were measured from the peak of one micelle to the peak of the next.

Table 2. Temperature Dependence of the Volume per Nanometer, Molecular Weight per Nanometer, and Aggregation Number per Nanometer for Wormlike Micelles

T (°C)	micelle V (nm^3/nm)	tip[a] V (nm^3/nm)	MW/nm (kDa/nm)	aggregation no. nm^{-1}
23	856 ± 29	536 ± 54	510 ± 36	10.1 ± 0.7
40	813 ± 26	653 ± 55	480 ± 26	9.6 ± 0.5
60	741 ± 12	231 ± 33	440 ± 24	8.8 ± 0.5

[a] The variation in the tip volume is due to the variation in tip radius.

sectional area added by the tip from the intercept, as seen in Figure 4. Once the cross-sectional area had been found, multiplying by the bulk density of the diblocks $\rho = 0.98$ g/cm^3 yields the linear density of the micelle. The aggregation number per unit length was then calculated by dividing the linear density by the molecular weight of the diblock. It was found by AFM that at a temperature of 40 °C the wormlike micelles have an aggregation number of 9.6 ± 0.5 nm^{-1}.

One should realize that AFM is a surface technique, and it is not able to probe voids that might exist between the micelles themselves, as illustrated in Figure 3A. It is possible that the polyisoprene in the micelles is able to flow slightly, filling in the voids between the micelles. This would help to explain why the heights are smaller than the diameters, as seen in Table 1. However, if by some chance there are voids between the micelles, the empty space would be counted as polymer volume, resulting in a larger aggregation number, which can be estimated to be about 15% higher. A second issue to consider is that the AFM measurements were done in a dry state. In the analysis the bulk density for the polymer was used. However, if the micelles are swollen with solvent after they have been adsorbed and allowed to dry, their density could be lower than the bulk density because of vitrification of the PS core. The lower core density would also cause the calculated aggregation number per nanometer to be larger. The last issue is that AFM can actually cause sample deformation. This would cause the measured cross-sectional area to be smaller than the actual area and would result in a smaller aggregation number. Therefore, it is possible that the errors due to voids and micelle deformation might partially cancel each other.

Aggregation Number from Static Light Scattering. In light scattering, the scattering wavevector, q is defined as $4\pi n/\lambda \sin(\theta/2)$, where n is the refractive index of the solvent, λ is the wavelength of light used, and θ is the scattering angle. When $qR_g < 1$, where R_g is the radius of gyration, the entire object can be studied by light scattering, yielding the R_g, hydrodynamic radius R_h (by dynamic light scattering), and the total weight-averaged molecular weight, M_W, of the micelle, from which the aggregation number can be calculated. This is not the case for the wormlike micelles, which were found, by AFM, to be very large, causing $qR_g > 1$. Thus, only the mass per unit length can be measured by static light scattering from the Holtzer[26] plot, in which $R_\theta q/$

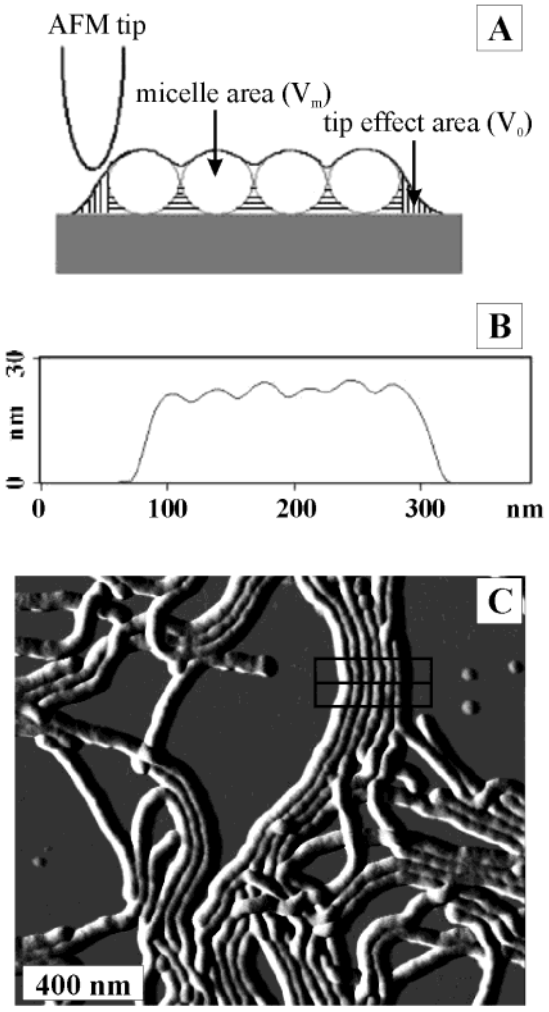

Figure 3. Image A is a cartoon image of tip broadening in AFM images while scanning across nanoscopic cylinders lying parallel to one another. The areas denoted with vertical stripes are areas added by the tip, which can be eliminated through our analysis. Depending on the tip shape, this area can be up to 80% of the micellar area. The areas denoted with horizontal stripes indicate where possible voids might exist. These voids are not eliminated during analysis but are less than 15% of the micellar volume. Image B is a cross-sectional profile along the line in image C, showing actual broadening of cylindrical micelles by the AFM tip. Image C is an AFM amplitude image of 40−10 micelles adsorbed from heptane at $T = 60$ °C. The box shows the subsection area in which the volume of six parallel micelles was calculated.

$Kc\pi$ is plotted as a function of q, where R_θ is the Rayleigh ratio, $K = 4\pi^2 n^2/\lambda^4 N_{Av}(dn/dc)^2$is the optical constant, N_{Av} is Avogadro's number, c is the concentration of polymer in solution, and dn/dc is the specific change in refractive index for a polymer solvent pair, which for 40−10 in heptane can be calculated[27] as 0.190. Dividing the plateau value in Figure 5, which is equal to the mass per unit length, by the molecular weight of the diblock gives the aggregation number per unit length. We can then compare the results from light scattering with those obtained from AFM. At a temperature of 40 °C, light scattering gives an aggregation number of 10.5 ± 0.3 nm^{-1}, which is in good agreement with the AFM value of 9.6 ± 0.5 nm^{-1}. As seen in Figure 6, for both the AFM and light scattering data it is clear that as the temperature is raised above 40 °C, the aggregation number per unit length decreases. This decrease is to be expected, since in this study heptane was used as the poor solvent for polystyrene: as the

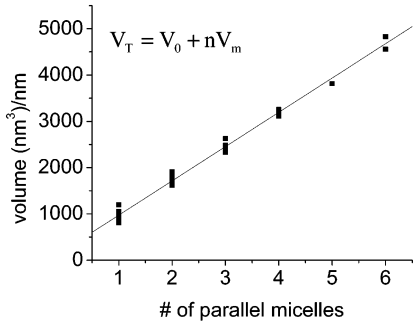

Figure 4. Plot of the total volume per nanometer (V_T) vs the number of parallel micelles (n) for 40−10 diblock adsorbed from heptane at $T = 60$ °C. The intercept gives the volume added by the tip (V_0), and the slope gives the volume per unit length for an individual micelle (V_m).

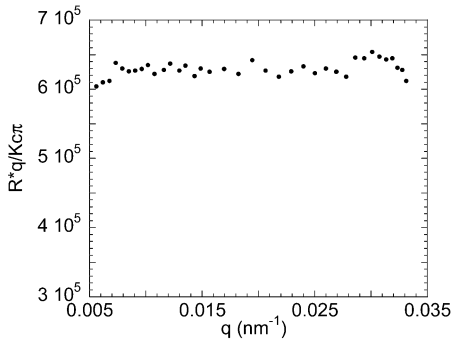

Figure 5. A representative Holtzer plot for 40−10, corresponding to a concentration of 3.5×10^{-5}g/mL, measured at 25 °C. The value of the plateau results in an aggregation number of 12 ± 0.2 nm^{-1}.

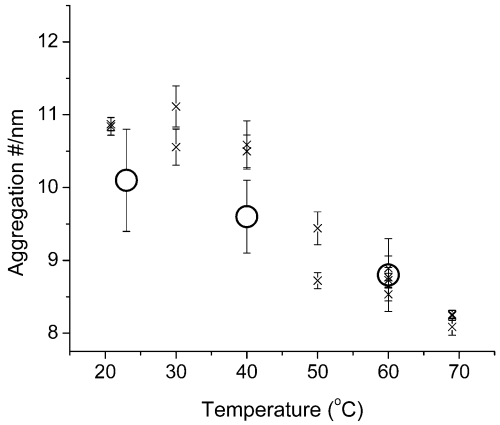

Figure 6. Variation of aggregation number per nanometer as a function of temperature. Circles and ×'s are AFM results and light scattering results, respectively.

temperature is raised, heptane becomes a better solvent, lowering the surface energy and allowing for smaller aggregation numbers. One would expect the aggregation number per unit length to increase at temperatures below 40 °C; however, it appears to level off and not increase further. As such, samples below 40 °C might not be in true equilibrium (possibly due to freezing of the swollen polymer core). Preliminary studies indicate above 45 °C equilibration appears to take place within a couple of hours; however, at lower temperatures the equilibration time is much longer. The equilibration of micellar solutions needs to be studied in greater detail.

Conclusions

From this work it is shown that wormlike micelles can be observed in dilute solutions of neutral and amorphous diblock copolymers in selective solvents. It is also shown that the aggregation number per unit length of these wormlike micelles decreases as the temperature is increased. By using a combination of AFM and light scattering, it was shown that adsorbing the micelles onto a surface does not significantly change their linear density. To this end, it is seen that AFM and light scattering complement each other nicely in studying wormlike micelles. From light scattering, one is able to study internal structure; from AFM, one is able to study properties of the entire micelle.

Acknowledgment. We thank Sharon L. Wells for the initial work she did on this project, E. B. Zhulina for useful discussions, the National Science Foundation NIRT ECS0103307 for funding, and the STC Program of the National Science Foundation under Agreement CHE-9876674 for funding and shared facilities.

Supporting Information Available: Figures showing molecular weight distributions obtained by GPC in THF of samples 1 and 2, intensity vs particle diameter measured for sample 1, and intensity vs particle diameter curves for sample 2. This material is available free of charge via the Internet at http://pubs.acs.org.

References and Notes

(1) Tuzar, Z.; Kratochvil, P. *Adv. Colloid Interface Sci.* **1976**, *6*, 201.
(2) Hamley, I. W. *The Physics of Block Copolymers*; Oxford Universtity Press: Oxford, England, 1998.
(3) Tuzar, Z.; Kratochvil, P. *Surf. Colloid Sci.* **1993**, *15*, 1.
(4) Halperin, A.; Tirrell, M.; Lodge, T. P. *Adv. Polym. Sci.* **1992**, *100*, 31.
(5) Chocair, A.; Eisenberg, A. *Eur. Phys. J. E* **2003**, *10*, 37.
(6) Zhulina, E. B.; Birshtein, T. M. *Polym. Sci. U.S.S.R.* **1985**, *27*, 570.
(7) Lairez, D.; Adam, M.; Carton, J.-P.; Raspaud, E. *Macromolecules* **1997**, *30*, 6798.
(8) Adam, M.; Carton, J.-P.; Corona-Vallet, S. Lairez, D. *J. Phys. II* **1996**, *6*, 1781.
(9) Gao, Z.; Varshney, S. K.; Wong, S.; Eisenberg, A. *Macromolecules.* **1994**, *27*, 7923.
(10) Zhulina, E. B.; Adam, M.; LaRue, I.; Sheiko, S. S.; Rubinstein, M. *Diblock Copolymers Micelles in a Dilute Solution*, to be published.
(11) It should be noted that there can be a slight change in the surface area per block, which would lower the free energy of the interface; however, this change is small enough to be disregarded.
(12) LaRue, I.; Adam, M.; Sheiko, S. S.; Rubinstein, M. *Polym. Mater. Sci. Eng.* **2003**, *88*, 236.
(13) Zhang, L.; Eisenberg, A. *J. Am. Chem. Soc.* **1996**, *118*, 3168.
(14) Spatz, J. P.; Moessmer, S.; Moeller, M. *Angew. Chem., Int. Ed. Engl.* **1996**, *35*, 1510.
(15) Massey, J. A.; Temple, K.; Cao, L.; Rharbi, Y.; Raez, J.; Winnik, M. A.; Manners, I. *J. Am. Chem. Soc.* **2000**, *122*, 11577.
(16) Won, Y. Y.; Davis, H. T.; Bates, F. S. *Science* **1999**, *283*, 960.
(17) Liu, G. J.; Yan, X. H.; Duncan, S. *Macromolecules* **2002**, *35*, 9788.
(18) Liu, G. J.; Yan, X. H.; Duncan, S. *Macromolecules* **2003**, *36*, 2049.
(19) Liu, G. J.; Li, Z.; Yan, X. H. *Polymer* **2003**, *44*, 7721.
(20) Price, C. *Pure Appl. Chem.* **1983**, *55*, 1563.
(21) May, S.; Ben-Shaul, A. *J. Phys. Chem. B* **2001**, *105*, 630.
(22) Edenfeld, K. M.; Jarausch, K. F.; Stark, T. J.; Griffis, D. P.; Russel, P. E. *J. Vac. Sci. Technol. B* **1994**, *12*, 3571.
(23) Vesenka, J.; Miller, R.; Henderson, E. *Rev. Sci. Instrum.* **1994**, *65*, 2249.
(24) Bustamante, C.; Keller, D. *Phys. Today* **1995** (Dec), 32.
(25) Sheiko, S. S. *Adv. Polym. Sci.* **2000**, *151*, 61.
(26) Holtzer, A. *J. Polym. Sci.* **1955**, *17*, 432.
(27) Outer, P.; Carr, C. I.; Zimm, B. H. *J. Chem. Phys.* **1950**, *18*, 830.

MA049845B